Acoustic-Structure Interaction Simulation of Differential Phase Sensor

J. H. Lee*
Department of Mechanical Engineering, American University of Sharjah, Sharjah, UAE
*Corresponding author: Department of Mechanical Engineering, American University of Sharjah, PO Box 26666, Sharjah, UAE, jinhyuk@aus.edu

Abstract: This paper describes the methodology in the feasibility study and development of a novel biommimetic hydro-acoustic sensor by finite element method (FEM). Fluid-structure interaction of the sensor system has been studied since the motion of the sensor and that of the fluid are not independent from each other and are dictated by the fluid loading effect which has two main effects in general. Firstly, the fluid mass loads the structure meaning that the structural natural frequencies are altered due to added mass. Secondly, acoustic radiation will be provided by additional fluid medium damping. In this paper, the half-power bandwidth method is used to estimate radiation damping based on the corresponding Q value from the frequency response. In COMSOL Multiphysics Module, the Acoustic and Structural physics were used. Background acoustic pressure is used as an input to the sensor and Perfectly Matched Layer is used to simulate the unbounded boundary to avoid the standing waves.

Keywords: acoustics, MEMS sensor, fluid-structure interaction, radiation damping, Q factor

1. Introduction

The idea of an application as a hearing device based on a parasitoid fly, *Ormia ochracea* has been studied extensively recently [1, 2]. This paper addresses another possible application as an underwater directional sensor. In order to study the feasibility of the sensor in fluid medium, it is necessary to investigate the fluid-structure interaction between the hydro-sensor and the fluid medium because this type of system becomes dynamically coupled between the fluid and the structure when the structure starts to vibrate in fluid such as water. When a sensor starts to vibrate in water, it causes fluid loading to the sensor which downshifts the natural frequency of the sensor and acoustic radiation is provided by the fluid medium as an additional damping. Vibrating structure in fluid, even in air, radiate sound, especially as frequency increases [3]. According to [3], a structure interacting with surrounding medium becomes a good radiator when the bending wave velocity in the structure equals the speed of sound in the fluid medium. However, our study shows that it still radiates substantial amount of the structural sound as additional damping even well below the critical frequency.

The outcome of the paper has two folds: Simulated results are used to validate the lumped parameter model of the sensor developed in [4] and are used to calculate sound radiation due to the vibration of the sensor in the fluid domain.

In this study, numerical simulation of the acoustically fluid-structure interaction has been performed which consists of an underwater sensor in fluid medium using COMSOL Multiphysics Module: The acoustic and structural physics have been used for a frequency domain analysis and for additional damping effect due to sound radiation.

2. Hydro-Acoustic Sensor

Fig. 1 (a) shows the two degrees of freedom (DOF) mechanical sensor model of parasitoid fly, *Ormia orchracea*. As shown in Fig. 1 (b), three dimensional finite element (FE) model with axes, the sensor looks like two thin plate are coupled together. This introduces the bad aspect ratio which brings difficulties in terms of the solution convergence and meshing when modeling and analyzing FE sensor model. To resolve this issue, two-dimensional analysis is chosen over three-dimensional one by taking advantage of symmetry.

Unlike a hydrophone array, which detects propagation direction by the arrival time of sound waves, this novel sensor is based on a mechanically-coupled mechanism which amplifies the time delay of the arriving sound wave. Regardless of the type of medium around the sensor, air or water, the fundamentals behind how the sensor works are the same. According to

[1], this type of sensor utilizes the first two modes of vibration to enhance the phase difference, hence the time delay of the sound wave signal impinging on the sensor. Fig. 2 shows the eigenmodes of the sensor in vacuo which correspond to the first and second eigenfrequencies: (a) out of phase and (b) in-phase modes.

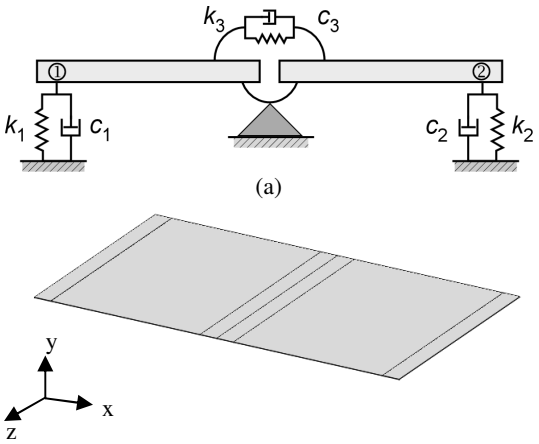

Figure 1. (a) Two degrees of freedom mechanical model of hearing system of parasitoid fly, *Ormia ochracea* and (b) three dimensional Finite Element Model with axes.

A lumped parameter model is derived for the sensor shown in Fig. 3 [4]. Since there are three DOF (two translations and one rotation) at each node, the total degrees of freedom of the sensor is 15. However, applying the boundary conditions (fixed-fixed along the sidelines and pinned at the centerline) and assuming that there is no in-plane displacement, the degrees of freedom is reduced to five. With the damping term the system of equation becomes

$$\mathbf{M_F}\ddot{\mathbf{u}}_\mathbf{F} + \mathbf{C_F}\dot{\mathbf{u}}_\mathbf{F} + \mathbf{K_F}\mathbf{u_F} = \mathbf{f_F} \qquad (1)$$

where $\mathbf{M_F}$ is the mass matrix with the fluid mass loading effect, $\mathbf{C_F}$ is the damping matrix, $\mathbf{K_F}$ is the stiffness matrix, $\mathbf{f_F}$ is the nodal load, and $\mathbf{u_F}$ is the nodal displacement of the sensor structure. The nodal load $\mathbf{f_F}$ is composed of the external driving forces, f_1 and f_2, which are due to the sound wave pressure impinging on each side of the sensor and can be calculated by

$$f_1 = sp_o e^{i\omega\tau/2} \qquad (2)$$

$$f_2 = sp_o e^{-i\omega\tau/2} \qquad (3)$$

where s is the surface area of each side of the plate and p_o is the magnitude of the impinging acoustic pressure wave, and τ is the time delay. In order to evaluate the effect of the impinging pressure wave on the response of the sensor structure, transfer functions are obtained as follows:

$$TF_1(\omega) = \frac{\det\left(\mathbf{K} - \mathbf{M}\omega^2\big|_{(,2)=\mathbf{f}}\right)}{\det\left(\mathbf{K} - \mathbf{M}\omega^2\right)} \qquad (4)$$

$$TF_2(\omega) = \frac{\det\left(\mathbf{K} - \mathbf{M}\omega^2\big|_{(,4)=\mathbf{f}}\right)}{\det\left(\mathbf{K} - \mathbf{M}\omega^2\right)} \qquad (5)$$

where $\mathbf{A}\big|_{(,j)=\mathbf{f}}$ represents a matrix $\mathbf{A}$ with the j-th column replace by a vector $\mathbf{f}$. Eq. (4) represents the effect of the pressure wave on the transverse motion of node 2, and Eq. (5) represents the effect of the pressure wave on the transverse motion of node 3 from Fig. 3.

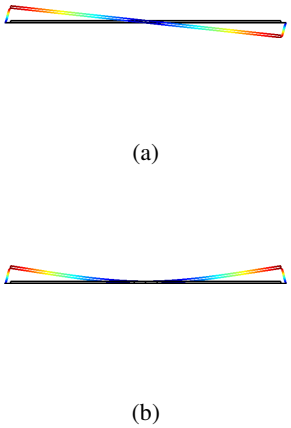

(a)

(b)

Figure 2. (a) First (rocking) and (b) second (bending) eigenmode shapes of the hydro-acoustic sensor.

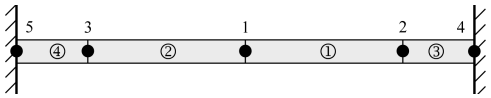

Figure 3. Representation of the hydro-acoustic sensor using four Euler-Bernouli Beam elements where numbers in circles represent elements and plain numbers represent nodes.

3. Use of COMSOL Multiphysics

The physical behavior of the 2D sensor in fluid domain is investigated using the commercial finite element software COMSOL. A 2D sensor model is built assuming plane strain by using the Structure Mechanics Module. The assumption of plane strain is made since the cross-sectional geometry of the sensor does not vary in one direction, and the loading does not vary in the same direction, hence there is assumed to be no in-plane strain along the z-direction in Fig. 1 (b).

The hydro-acoustic sensor is made of a Polysilicon plate that is allowed to tilt along the centerline by a supporting structure. The two sides of plate are attached to the sensor housing through two narrow strips of PDMS (polydimethylsiloxane), which allows both rotational and transverse motions of the sideline of the structure. The polysilicon plate acts as a sensor and PDMS strip acts as a linear spring k_1 and k_2 shown in Fig. 1. The structure and material properties of the hydro-acoustic sensor are provided in Table 1.

Table 1: Structure and material properties of the hydro-sensor (Numbers in circles represent the elements shown in Fig. 3).

Material	Polysilicon ①②	PDMS③④
Thickness *t*	19μm	2μm
Modulus of Elasticity *E*	160GPa	8.7MPa
Density *ρ*	2320	483
Poisson ratio *v*	0.22	0.499
Beam length *L*	1.2mm	0.5μm
Beam width *w*	1.2mm	1mm

3.1 Governing equations

It is possible to describe the strain conditions at a point with the deformation components u, v and their derivatives due to the plain strain assumption. For the small displacement assumption, the general definitions of normal and shear strains are given from the deformation as

$$\varepsilon_x = \frac{\partial u}{\partial x}$$
$$\varepsilon_y = \frac{\partial u}{\partial y} \qquad (6)$$
$$\gamma_{xy} = \frac{\partial u}{\partial y} + \frac{\partial v}{\partial x}.$$

The strains given by Eqs. (6) are represented by the vector column matrix as

$$\{\varepsilon\} = \begin{Bmatrix} \varepsilon_x \\ \varepsilon_y \\ \gamma_{xy} \end{Bmatrix}. \qquad (7)$$

Applying the plain strain condition $\varepsilon_z = \gamma_{xz} = \gamma_{yz} = 0$ to the three-dimensional stress/strain relationship, the relationship for linear condition is

$$\sigma = D\varepsilon, \qquad (8)$$

where

$$D = \frac{E}{(1+\nu)(1-2\nu)} \begin{bmatrix} 1-\nu & \nu & 0 \\ \nu & 1-\nu & 0 \\ 0 & 0 & \frac{1-2\nu}{2} \end{bmatrix} \qquad (9)$$

is called the constitutive matrix, E is the modulus of elasticity, and v is Poisson's ratio. Considering force and moment equilibrium, the equilibrium equations expressed in the stresses are

$$-\frac{\partial \sigma_x}{\partial x} - \frac{\partial \tau_{yz}}{\partial y} = F_x$$
$$-\frac{\partial \tau_{xy}}{\partial x} - \frac{\partial \sigma_y}{\partial y} = F_y \qquad (10)$$
$$\sigma_{yx} = \sigma_{xy},$$

where F denotes the body forces.

For the Acoustics Module in which the acoustic pressure p is the basic dependent variable, the mathematical models of sound waves in a lossless medium can be represented with respect to the acoustic pressure p as

$$\frac{1}{\rho_0 c_s^2}\frac{\partial^2 p}{\partial t^2} + \nabla \cdot \left(-\frac{1}{\rho_0}(\nabla p) \right) = 0, \qquad (11)$$

where ρ_0 refers to the fluid density, c_s denotes the speed of sound of the fluid. Considering a time-harmonic wave, for which the pressure varies with time as

$$p(\mathbf{x},t) = p(\mathbf{x})e^{i\omega t} \quad (12)$$

where $\omega = 2\pi f$ is the angular frequency, with f denoting the frequency, Eq. (11) reduces to an Helmholtz equation:

$$\nabla \cdot \left(-\frac{1}{\rho_0}(\nabla p) \right) - \frac{\omega^2 p}{\rho_0 c_s^2} = 0 \quad (13)$$

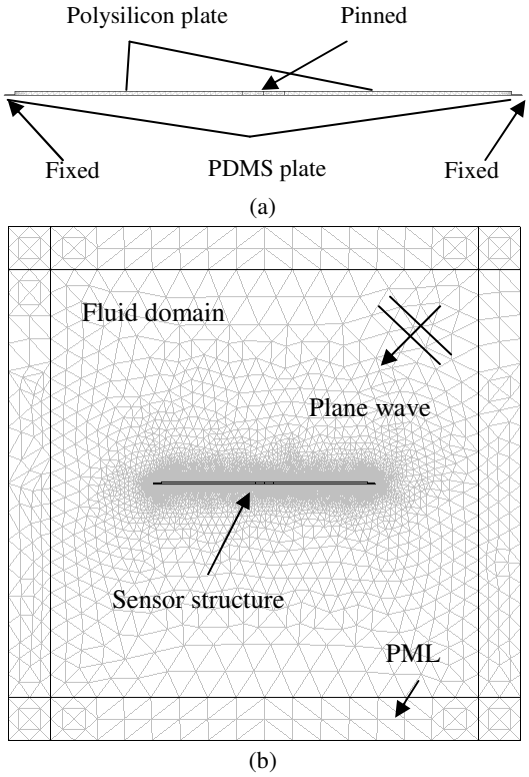

Figure 4. (a) Sensor model with material and boundary conditions, and (b) the global finite element model.

3.2 Geometry

As shown in Fig. 4 (a), the sensor structure consists of two polysilicon plates being coupled at the mid-point which is pinned and each end is attached to the PDMS plate which is fixed at its farther end from the sensor structure. Fig. 4 (b) shows that the background pressure is used to generate a plane wave coming from 45 degree angle. The source of the plane wave p_i is a scalar variable, which is introduced into the model as

$$p_i = e^{-i(k_x x + k_y y)}, \quad (14)$$

where $kx = k\cos\theta$, $ky = k\sin\theta$, x and y are the Cartesian coordinates. In Eq. (14), k is wavenumber.

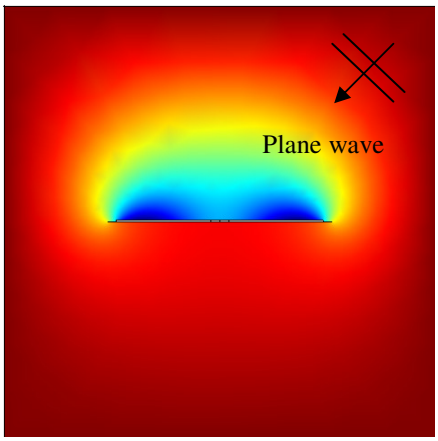

Figure 5. Post processing plot of the total acoustic pressure at 5000 Hz.

3.3 Boundary conditions

As shown in Fig. 4 (b) and Fig. 5, the background pressure field is used to provide a load (sound wave) to the sensor structure, and the structure provides accelerations to the surrounding medium. In Fig. 4 (b), acoustic fluid subdomain is modeled as a square area. The square area is in turn enclosed by rectangular areas that act as a perfectly matched layer (PML). The PML is used to absorb acoustic energy, to simulate a free field effect, thereby eliminating acoustic energy being reflected back into the square area from the square's outer boundary. Hence, the fluid medium is assumed to be unbounded (a sensor submerged in an infinite area of fluid) to avoid standing waves and not to sustain natural frequencies. It simply mass-loads the sensor, and provides acoustic radiation damping which will be calculated in the section 4.

All domains are meshed by Free Triangle elements. They are chosen based on the patch analysis which was performed for both triangle and quadrilateral elements. The analyses show that the result is not sensitive to the type of elements. The global model is composed of 224,984 elements.

Acoustic fluid domain is modeled as water with a density of 995.6 kg/m^3, the speed of sound of 1482 m/s. To couple the acoustic pressure

wave to the sensor structure, the boundary load is set on the structure as

$$F = -n_s \cdot p\,, \tag{15}$$

where n_s is the outward pointing unit normal vector. In order to couple the frequency response of the sensor back to the acoustic problem, the boundary condition of the normal acceleration a_n is set to equal to that of the sensor as

$$a_n = -n_a \cdot \left(-\frac{1}{\rho_0}\nabla p\right), \tag{16}$$

where n_a is the outward pointing unit normal vector. The equation for the interaction between the fluid and the structure is derived from the continuity requirement at the interface boundary. The normal displacement of the structure must be identical to that of the fluid. The fluid-structure interface equation is

$$\{n\}\cdot\{\nabla p\} = -\rho_0 \cdot \{n\}\cdot\frac{\partial^2 U}{\partial t^2}\,, \tag{17}$$

where U is the displacement vector of the structure at the interface.

4. Acoustic Radiation Damping

The governing equation which utilizes Rayleigh damping for our case is shown in Eq. (1) where the Rayleigh damping model is represented as:

$$\mathbf{C_F} = \alpha_{dM}\mathbf{M_F} + \beta_{dK}\mathbf{K_F}\,. \tag{18}$$

In Eq. (18), α_{dM} and β_{dK} are the mass and stiffness damping parameters, respectively. These parameters are usually not available in the literature; however the damping ratio can be calculated from the frequency response shown in Fig. 6 based on the Half-power bandwidth method. The damping ratio ξ for a specified pair of Rayleigh parameters, α_{dM} and β_{dK}, at the frequency f is

$$\xi = \frac{1}{2}\left(\frac{\alpha_{dM}}{2\pi f} + \beta_{dK}\,2\pi f\right). \tag{19}$$

Using Eq. (19) at two frequencies, f_1 and f_2, with different damping ratios, ξ_1 and ξ_2, results in an equation that can be solved for the Rayleigh parameters.

$$\begin{bmatrix}\xi_1\\ \xi_2\end{bmatrix} = \begin{bmatrix}\dfrac{1}{4\pi f_1} & \pi f_1\\ \dfrac{1}{4\pi f_2} & \pi f_2\end{bmatrix}\begin{bmatrix}\alpha_{dM}\\ \beta_{dK}\end{bmatrix} \tag{20}$$

The damping ratios for the sensor model in the water are found to be 0.0063 and 0.1235. There are corresponding Rayleigh parameters: α_{dM} = 4.0465 and β_{dK} = 9.0943e-6.

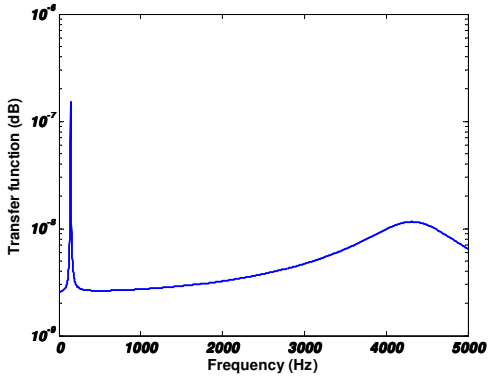

Figure 6. Frequency response of the sensor in water.

In order to capture only the acoustic radiation damping, other damping, such as internal and viscous, has not been chosen for the simulation.

5. Results

Numerical simulation yields an ideal response with respect to the fluid loading effect, and acoustic damping.

5.1 Fluid loading effect

Due to the added mass effect induced by the surrounding water, a significant decrease of the natural frequencies is observed. In Table 2, the comparison of the simulation is made *in vacuo* and in water up to 2nd natural frequencies.

The fluid added mass effect is estimated by calculating the frequency reduction ratio δ of each natural frequency defined as

$$\delta = \frac{(f_v - f_w)}{f_v} \tag{21}$$

where f_v and f_w are the natural frequencies *in vacuo* and in air. It can be observed that the natural frequencies are considerably reduced by the presence of fluid. It also shows that the

frequency reduction ratio does not remain constant, and rather decreases as the frequency increases.

Table 2: Comparison for *in vacuo* and in water natural frequencies of the hydro-sensor

Natural frequencies	1st natural frequency	2nd natural frequency
In vacuo	870 Hz	18469 Hz
In water	137 Hz	4300 Hz
Percentage decrease	84 %	74 %

5.2 Validating lumped model and acoustic damping

The simulated result has been compared to the lumped parameter model developed in [4] to validate the model. Fig. 7 shows that the comparison between the lumped parameter and FE model is agreeable to each other.

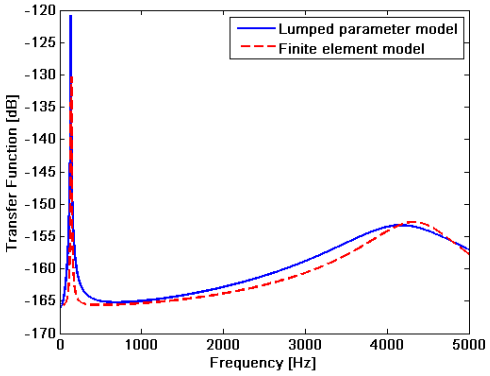

Figure 7. Comparison of frequency responses by FE and lumped parameter models for a sensor in water.

The fluid appears to be the structure like an added mass which means that the fluid pressure on the wet surface is in phase with structural acceleration at low frequencies. The fluid impedance becomes complex at higher frequencies, since it involves both mass-like and damping like effects. For the reason, α_{dM} is set to zero whereas β_{dK} is set to the value calculated based on the Half-power method (β_{dK} = 9.0943e-6).

According to [3], the structure only becomes a good radiator at or above the critical frequency. However, it is shown that the structure in water like medium radiates sound energy even in low frequencies and the sound radiation increases as frequency increases as a form of damping.

6. Conclusions

In this paper, an acoustically fluid-structure model of the sensor has been simulated using COMSOL Multiphysics software. It was used to validate the lumped parameter sensor model developed in [4] and to calculate the damping ratio as well as its coefficient by simulating sound radiation due to fluid-structure interaction. It is concluded that the sound radiation damping cannot be overlooked in designing a sensor since it produces substantial amount of damping.

The numerical techniques presented in this paper can be utilized in various ways: (1) feasibility study of the sensor, (2) validation of the sensor model due to geometry changes, (3) calculating the added mass due to fluid loading, and (4) calculating extra damping in fluid due to sound radiation.

9. References

1. Miles, R. N., Robert, D., and Hoy, R. R., Mechanically coupled ears for directional hearing in the parasitoid fly Ormia ochracea, *J. Acoust. Soc. Am.*, **98(6)**, 3059-70 (1995)

2. Miles, R. N., *et al.*, Design of a Biologically Inspired Directional Acoustic Sensor, *Meeting of the MSS Specialty Group on Battlefield Acoustic and Seismic Sensing, Magnetic and Electric Field Sensors*, Volume **I**: Special Session Held 23 October (2001)

3. Norton, M. and karczub, D., *Fundamentals of Noise and Vibration Analysis for Engineers*, 197-203. Cambridge University Press, UK (2003)

4. Lee, J., *et al.*, Modeling and Characterization of Bio-Inspired Hydro-Acoustic Sensor, *Journal of Acoustics and Vibrations*, VIB-14-1182, in review (2014)